Co-published by
Institute of Fluid-Flow Machinery
Polish Academy of Sciences
Committee on Thermodynamics and Combustion
Polish Academy of Sciences

http://www.imp.gda.pl/archives-of-thermodynamics/

Convection and heat transfer analysis of Cu-water rotatory flow with non-uniform heat source

Alfunsa Prathiba[a*], P. Johnson Babu[b], Manthri Sathyanarayana[c], B. Tulasi Lakshmi Devi[d], Shanker Bandari[e]

[a]Department of Mathematics, CVR College of Engineering, Hyderabad, India
[b]Department of Physics and Electronics, St. Joseph's Degree & PG College, 5-9-1106 King Koti, Main Road, Hyderabad - 500029, Telangana, India
[c]Department of Mathematics & Statistics, St.Joseph's Degree & PG College, 5-9-1106 King Koti, Main Road, Hyderabad - 500029, Telangana, India
[d]Department of Mathematics, Koneru Lakshmaiah Education Foundation, Telangana, India
[e]Department of Humanities and Sciences, CVR College of Engineering, Telangana, India
*Corresponding author email: alphonsaperli@gmail.com

Received: 29.11.2023; revised: 23.02.2024; accepted: 10.06.2024

Abstract

This article explores the phenomenon of natural convection in the rotatory flow of Cu-water nanofluid under the influence of non-uniform heat source. In order to design more effective and efficient cooling systems, this work attempts to increase our understanding of how nanofluids behave in the presence of non-uniform heat sources, convection, and rotatory force. The higher order partial differential equations governing the flow are remodelled into ordinary differential equations using similarity transformations. The remodelled equations were solved using shooting methodology and the Lobatto-III A algorithm. The impacts of various parameters such as the Richardson number ($1 < Ri < 4$), the Schmidt number ($0.5 < Sc < 2$), nanoparticle's volume fraction ($0.02 < \phi < 0.08$), etc. on velocity, concentration and temperature was analysed. One of the main findings of this analysis was study of the impact of the space dependent heat source ($0.2 \leq A \leq 1$) and the temperature dependent internal heat source ($0 \leq B \leq 0.5$) on the heat regulation. Furthermore, increasing the quantity of the nano-additives and improving the fluid's thermophysical properties intensified the acceleration of the fluid elements in the flow region. The presence of spatial and temperature-sensitive parameters facilitated quantification of the effects of a standard and variable heat source in combination of Coriolis force in the case of a Cu-water flow. The findings of the investigation will be helpful in the process of medical, architectural planning systems, oil recovery systems and so on.

Keywords: Coriolis force; Lobatto IIIA technique; Richardson number; Volume fraction of Cu nanoparticle; Non-uniform heat source

Vol. 45(2024), No. 3, 149–157; doi: 10.24425/ather.2024.151225

Cite this manuscript as: Prathiba, A., Babu, P.J., Sathyanarayana, M., Devi, B.T.L., & Bandari, S. (2024), Convection and heat transfer analysis of Cu-water rotatory flow with non-uniform heat source. *Archives of Thermodynamics*, 45(3), 149–157.

1. Introduction

The heat transmission process in nanofluids is important for many industrial and manufacturing applications. Initially, a sizable number of engineering applications relied solely on traditional heat transfer agents. However, currently they are used in intense cooling processes [1]. Further, the unique characteristic of matter at the nanoscale in nanotechnology has become a pop-

Nomenclature

A – coefficient of space dependent source/sink
a – constant ($a > 0$)
B – coefficient of temperature dependent heat source/sink
C – concentration of the species
C_p – specific heat at constant pressure constant pressure, J kg^{-1}K^{-1}
C_w – free stream concentration
C_∞ – uniform constant concentration
D – mass diffusivity coefficient
$\bar{g}$ – gravitational acceleration, m s^{-2}
k – thermal conductivity, W m^{-1}K^{-1}
Pr – Prandtl number
q''' – rate of internal heat generation/absorption
R_0 – rotational parameter
Re – Reynolds number
Ri – Richardson number
Sc – Schmidt number
T – fluid temperature, K
T_w – surface temperature, K
T_∞ – ambient temperature, K
U_w – free flow velocity
u, v, w– x, y, z components of velocity, m s^{-1}
x, y, z– Cartesian coordinates, m

Greek symbols

β – thermal expansion coefficient, K^{-1}
ν – kinematic viscosity, m^{2}s^{-1}
ϕ – nanoparticle's volume fraction
ρ – fluid density, kg m^{-3}
Ω – angular velocity, rad s^{-1}
μ – dynamic viscosity, kg m^{-1}s^{-1}
η – similarity variable
Θ – dimensionless temperature
Φ – dimensionless concentration

Subscripts and Superscripts

f – fluid
nf – nano fluid
s – solid particle
w – condition at wall
∞ – ambient condition
' – differentiation with respect to η

Abbreviations and Acronyms

MHD– magnetohydrodynamic

ular research topic in the twenty-first century. This resulted due to the limitations of thermal conduction of the aforementioned agents. Heat transfer efficiency can be considerably enriched by including metallic and non-metallic particles in ordinary fluids. The rise in the thermal conductivity of nanofluid has spurred a flurry of activity in the field of flow analysis. The thermal conductivity of several common fluids, such as water, toluene, ethylene glycol and mineral oils, is negligible. To overcome the issue of lower thermal conductivity of the above mentioned fluids Choi introduced the suspension of nanometre-sized particles (10–100 nm) or fibres into the conventional fluids [2]. To put it another way: nanoparticle-encapsulated fluids offer superior gripping, dispersion and scattering capabilities when applied to a solid substrate. Nanofluids have been the subject of much study for applications in engineering and manufacturing, especially as heat transfer fluids. These nanoparticle-containing fluids have many uses in a wide range of industries [2]. Scholars have examined several facets of nanofluids, such as enhancing thermal conductivity, integrating nanoparticles, and other associated domains [2–5].

Convective heat transfer in nanofluid has multiple uses and is essential in research and engineering [6]. Nanofluids are practically used in every technology that requires heat transfer agents for temperature control, such as renewable radiation, nuclear reactors, etc. As a result, fluid dynamics experts have paid particular attention to the field of nanofluids in recent years, owing to potential applications in various sectors [7].The influence of an exogenous directed magnetic force on heat exchange and entropy formation of nanofluid flow of Cu-water in a heated open cavity from beneath was investigated numerically by Mehrez et al. [8]. Punith Gowda et al. [9] explored the steady Marangoni driven boundary layer flow, mass and heat transfer properties of a nanofluid. Their findings indicate that strengthening the Marangoni number upgrades the flow velocity and lowers heat transfer. Yacob et al. [7] examined the steady 3D flow across a rotating extending/diminishing sheet fluid containing SCNT (single-walled carbon nanotubes) and MCNTs (multi-walled carbon nanotubes) in kerosene and water as base fluids. Faisal Shahzad et al. [10] studied the Fe_2O_4-H_2O flow sandwiched between two gyrating plates, presuming porosity in the top side, in order to create forced convection, the bottom surface was assumed to move at a variable speed. Through their meticulous analysis, Ashraf et.al. forecasted how heat and fluid would move around a non-conducting horizontal circular cylinder implanted in a porous material at various angles [11].

The magneto-thermoanalysis of electrically conducting flow over the vertically symmetric heated plate using the Keller box method was done by Ullah et al. [12]. Further, the importance of the convective heat transfer with various fluids in different conditions and flow regimes can be learned from the papers [13–17].

The exploration of heat production or absorption impacts the moving fluids. It is crucial due to various physical issues. With the rapid advancement of digital means, adequate refrigeration of electrical devices have become necessary. This equipment includes everything from single transistors to mainframe computers, energy suppliers, and telephone switchboards [18]. Hasarika et al. [4] in their theoretical investigation using the perturbation technique examined the impact of the nanoparctical volume fraction along with thermo-diffusion on a chemically retorting MHD (magnetohydrodynamic) Cu-water fluid flow. They discovered that "cupper particles had a better conductivity than

water based particles". And a noteworthy finding in their study is that the flow velocities are increased due to the influence of internal heat, diffusion and core heat generation.

One of the most important factors in changing the direction of fluid flow is the Coriolis force [19]. It is equivalent to other inertial forces such as magnetohydrodynamic forces and viscous forces in the fundamental equations of fluid dynamics. Liquid flow on the surface of the Earth is influenced by a number of forces, including friction, centrifugal, gravitational and pressure gradient forces. On the other hand, the Coriolis force usually has little effect on transport phenomena in the situations of atmosphere and water. This is most noticeable when the liquid motion speed is much slower than the rotating speed, which makes the Coriolis effect insignificant and the reason it is not commonly noticed on Earth. However, studies on the Coriolis force's effects on various liquid streams have been conducted in recent decades and each of these analyses have identified that this force has a significant impact of the flow velocities [20–22].

The analysis of the current research has been done based on the above literature assessment. As per the gap identified by the authors, the impact of non-uniform heat on rotatory nanofluid flow has not been investigated in any methodical paper. Thus, the prime objective of this paper is to analyse the predominance of a non-uniform heat source and convective rotatory flow of Cu-water nanofluid across a stretched sheet. Typical applications for rotating flows include centrifugal filtering, cooling high-speed aircraft skins, anticyclone flow circulation, and the geological stretching of tectonic plates under rotating oceans [2].

2. Problem formulation

A steady, incompressible nanofluid rotating flow over an elongating sheet under the stimulus of convection in the presence of a non-uniform source or sink has been considered for this study [23]. Its basic prototype of the flow is demonstrated in Fig. 1. The rotatory nanofluid flow is considered in the region $z \geq 0$. The *xy*-plane is anticipated to be linearly stretching in the direction of the flow with the free flow velocity $U_w = ax$, where $a > 0$ is a constant. The fluid is a copper-comprising water-based nanofluid. This two-component mixture flow is assumed under the following conditions [24]:

a) no chemical reaction,

b) minimal amount of viscous dissipation,

c) insignificant radiative heat transportation,

d) ensuring that there is no slip between the base fluid H_2O, and the nanoparticles (Cu) and that they are in thermal equipoise [24].

Centred on the above hypotheses, the governing equations of the flow are [25,26]:

$$\frac{\partial u}{\partial x}+\frac{\partial v}{\partial y}+\frac{\partial w}{\partial z}=0, \tag{1}$$

$$u\frac{\partial u}{\partial x}+v\frac{\partial u}{\partial y}+w\frac{\partial u}{\partial z}=\frac{\mu_{nf}}{\rho_{nf}}\frac{\partial^2 u}{\partial z^2}+2\Omega v+\bar{g}\beta_{nf}(T-T_\infty), \tag{2}$$

$$u\frac{\partial v}{\partial x}+v\frac{\partial v}{\partial y}+w\frac{\partial v}{\partial z}=\frac{\mu_{nf}}{\rho_{nf}}\frac{\partial^2 v}{\partial z^2}-2\Omega u, \tag{3}$$

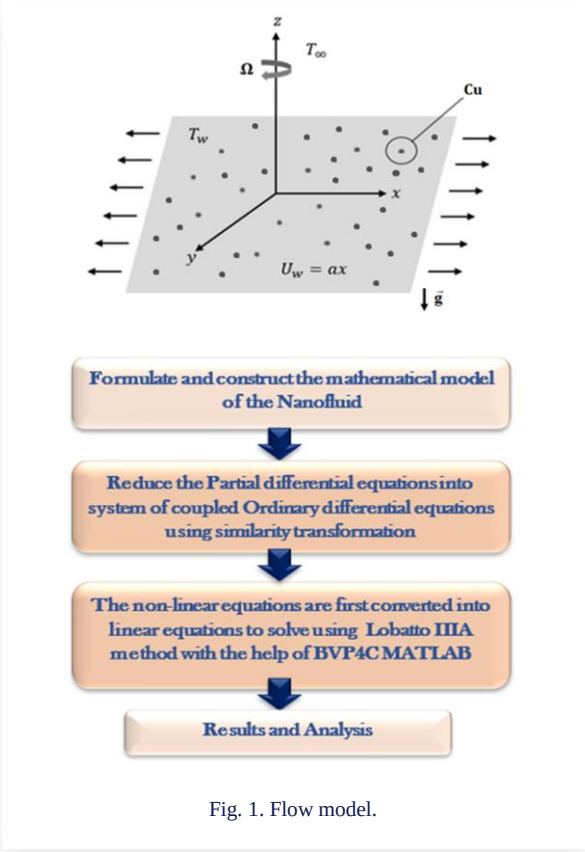

Fig. 1. Flow model.

$$u\frac{\partial T}{\partial x}+v\frac{\partial T}{\partial y}+v\frac{\partial T}{\partial z}=\frac{k_{nf}}{(\rho C_p)_{nf}}+\frac{q'''}{(\rho C_p)_{nf}}\tau, \tag{4}$$

$$u\frac{\partial C}{\partial x}+v\frac{\partial C}{\partial y}+w\frac{\partial C}{\partial z}=D_{nf}\frac{\partial^2 C}{\partial z^2}. \tag{5}$$

The boundary conditions are:

$$u=U_w,\ v=0,\ w=0,\ T=T_w,\ C=C_w\ \text{ as }\ z\to 0,$$
$$u\to 0, v\to 0, w\to 0,\ T\to T_\infty; C\to C_\infty\ \text{ as }\ z\to\infty, \tag{6}$$

where (u,v,w) are velocity components along the *x*-, *y*-, and *z*-directions, respectively, T and C are the temperature and concentration, $\bar{g}$ is the gravitational acceleration, and μ_{nf} is the dynamic viscosity [2]; ρ_{nf} is the density, k_{nf} is the thermal conductivity, $(\rho\beta)_{nf}$ is the thermal expansion coefficient of nanofluid [2], q''' is the rate of internal heat generation/absorption [27], $(\rho Cp)_{nf}$ is the heat capacitance, D_{nf} is the mass diffusivity [28] of the nanofluid, which are given by:

$$q''' = \frac{\alpha_f U_w}{x\nu_f}[A(T_w-T_\infty)f'(\eta)+B(T-T_\infty)],$$

$$\mu_{nf}=\frac{\mu_f}{(1-\phi)^{5/2}},$$

$$\rho_{nf}=(1-\phi)\rho_f+\phi\rho_s,$$

$$k_{nf}=k_f\left[\frac{k_s+2k_f-2\phi(k_f-k_s)}{k_s+2k_f+\phi(k_f-k_s)}\right],$$

$$(\rho C_p)_{nf}=(1-\phi)(\rho C_p)_f+\phi(\rho C_p)_s,$$

$$(\rho\beta)_{nf} = (1-\phi)(\rho\beta)_f + \phi(\rho\beta)_s,$$

$$D_{nf} = \frac{D_f}{1-\phi}. \quad (7)$$

The subscripts *nf*, *f* and *s* indicate the properties of nanofluid, base fluid ($\phi = 0$),and the solid nanoparticle. ϕ is the 'significant volume fraction of the nanoparticle' of (Cu), *A* and *B* are the coefficients of 'space and temperature-dependent heat source/sink', respectively [27]. The condition $A, B > 0$ relates to 'internal heat generation' and $A, B < 0$ corresponds to 'internal heat absorption' [27].

Let us consider the following similarity transformations [7]:

$$\eta = \sqrt{\frac{a}{v}}z,\ u = axF'(\eta),\ v = axG(\eta),\ w = -\sqrt{av}F(\eta),$$

$$\Theta(\eta) = \frac{T-T_\infty}{T_w-T_\infty},\ \Phi(\eta) = \frac{C-C_\infty}{C_w-C_\infty}. \quad (8)$$

The above transformation completely satisfies Eq. (1) and Eqs. (2)–(5), along with the boundary conditions, Eqs. (6), transformed into highly non-linear ordinary differential equations (ODEs), which can be given as:

$$\frac{\mu_{nf}}{\mu_f}\frac{\rho_f}{\rho_{nf}}F''' + \frac{\beta_{nf}}{\beta_f}\mathrm{Ri}\Theta = (F')^2 - FF'' - 2R_0G, \quad (9)$$

$$\frac{\mu_{nf}}{\mu_f}\frac{\rho_f}{\rho_{nf}}G'' = F'G - G'F + 2R_0F, \quad (10)$$

$$\frac{k_{nf}}{k_f}\frac{(\rho C_p)_f}{(\rho C_p)_{nf}}[\Theta'' + AF' + B\Theta] + \mathrm{Pr}F\Theta' = 0, \quad (11)$$

$$\Phi'' + \frac{\mathrm{Sc}}{(1-\phi)}F\Phi' = 0, \quad (12)$$

with the boundary conditions:

$$F'(\eta) = 1,\ G(\eta) = 0,\ F(\eta) = 0,\ \Theta(\eta) = 1,\ \Phi(\eta) = 1 \text{ at } \eta = 0,$$

$$F'(\eta) \to 0,\ G(\eta) \to 0,\ \Theta(\eta) \to 0,\ \Phi(\eta) \to 0 \text{ as } \eta \to \infty. \quad (13)$$

The parameters involved in the above equations are:

- rotational parameter: $R_0 = \frac{\Omega}{a}$,
- Prandtl number: $\mathrm{Pr} = \frac{v_f}{a_f}$,
- Schmidt number: $\mathrm{Sc} = \frac{v_f}{D_f}$.

The expression for the local drag force coefficients C_{fx} and C_{fy}, heat transfer coefficient Nu_x and the mass transfer coefficient Sh_x can be defined as:

$$C_{fx} = \frac{\tau_{xz}}{\frac{1}{2}\rho U_w^2},\quad C_{fy} = \frac{\tau_{yz}}{\frac{1}{2}\rho U_w^2},$$

$$\mathrm{Nu}_x = \frac{xq_w}{k(T_w-T_\infty)},\ \mathrm{Sh}_x = \frac{xq_m}{D_M(C_w-C_\infty)},$$

in which τ_{xz}, τ_{yz} indicate the shear stress and q_w, q_m represent the heat and mass flux at the walls of the sheet. Applying the transformations, Eqs. (8), the above expressions are transformed into:

$$\mathrm{Re}_x^{1/2}C_{fx} = \frac{\mu_{nf}}{\mu_f}F''(0),\quad \mathrm{Re}_x^{1/2}C_{fy} = \frac{\mu_{nf}}{\mu_f}G'(0),$$

$$\mathrm{Re}_x^{-1/2}\mathrm{Nu}_x = -\frac{k_{nf}}{k_f}\Theta'(0),\ \mathrm{Re}_x^{-1/2}\mathrm{Sh}_x = -\frac{D_{nf}}{D_f}\Phi'(0). \quad (14)$$

3. Methodology of the solution

Equations (9) to (12) combined with the boundary conditions are solved by implementing the Lobatto IIIA method using BVP4C numerical code in the MATLAB software [30]. To implement this method, the non-linear equations are first converted into linear equations by opting the following procedure and then converting the equations compatible to be solved by the MATLAB code:

$$f_1 = F,\quad f_2 = F',\quad f_3 = F'',$$

$$F''' = f_3' = -A_1A_2[f_1f_3 + 2R_0g_1 - (f_2)^2 + A_4\mathrm{Ri}\Theta_1],$$

$$g_1 = G,\ g_2 = G',\ G'' = g_2' = A_1A_2[-f_1g_2 + 2R_0f_1 + f_2g_1],$$

$$\theta_1 = \Theta(\eta),\ \theta_2 = \Theta'(\eta),$$

$$\theta_3 = \theta_2' = -\frac{\mathrm{Pr}k_f}{k_{nf}}[A_3f_1\theta_2] - Af_2 - B\theta_1, \quad (15)$$

$$\Phi_1 = \Phi,\ \Phi_2 = \Phi',\ \Phi_3 = -\frac{\mathrm{Sc}f\Phi'}{(1-\phi)},$$

$$A_1 = \frac{\mu_f}{\mu_{nf}},\ A_2 = \frac{\rho_{nf}}{\rho_f},\ A_3 = \frac{(\rho C_p)_{nf}}{(\rho C_p)_f},\ A_4 = \frac{(\beta)_{nf}}{(\beta)_f}. \quad (16)$$

The modified boundary conditions are:

$$f_1 = 0,\ f_2 = 1,\ g_1 = 0,\ \theta_1 = 1,\ \Phi_1 = 1 \text{ as } \eta \to 0,$$

$$f_2 \to 0,\ g_1 \to 0,\ \theta_1 \to 0,\ \Phi_1 \to 0 \text{ as } \eta \to \infty. \quad (17)$$

The thermophysical properties of nanoparticles and base fluid are placed in Table 1, these values have been utilised to calculate the values mentioned in Eqs. (16).

Table 1. Physical property parameters used for the analysis [4].

Properties	Base fluid (water)	Nano-particles (Cu)
Thermal conductivity, k ($\mathrm{Wm^{-1}K^{-1}}$)	0.613	400
Density, ρ ($\mathrm{kgm^{-3}}$)	997.1	8933
Specific heat, C_p ($\mathrm{Jkg^{-1}K^{-1}}$)	4179	385
Thermal expansion coeff., β ($\mathrm{K^{-1}}$)	36.2×10^{-5}	1.67×10^{-5}

The MATLAB BVP4C programme implements the Lobatto IIIA collocation Runge-Kutta (RK) method [31]. The code was validated by calculating the values of C_{fx}, C_{fy} and Nu_x for the base fluid when $R_0 = 0, 0.5, 1, 2$. These obtained values were then compared with the previously published findings in Tables 2 and 3. The results demonstrate a strong agreement between the obtained results and the exiting literature.

Table 2. Comparison of the values of $\mathrm{Re}_x^{1/2}C_{fx}$ and $\mathrm{Re}_x^{1/2}C_{fy}$ for base fluid when ϕ = Ri = A = B = Sc = 0.

	Salleh et al. [7]		Present findings	
R_0	$\frac{\mu_{nf}}{\mu_f}F''(0)$	$\frac{\mu_{nf}}{\mu_f}G'(0)$	$\frac{\mu_{nf}}{\mu_f}F''(0)$	$\frac{\mu_{nf}}{\mu_f}G'(0)$
0.00	-1.00000	0.00000	-1.000000	0.000000
0.50	-1.13838	-0.51276	-1.138411	-0.512802
1.00	-1.32503	-0.83809	-1.325031	-0.837121
2.00	-1.65240	-1.28726	-1.652392	-1.287301

Table 3. Comparison of calculated values of $\mathrm{Re}_x^{-1/2}\mathrm{Nu}_x$ for base fluid.

	Nadeem et al. [32]	Salleh et al. [7]	Current findings
R_0	$\frac{-k_{nf}}{k_f}\Theta'(0)$	$\frac{-k_{nf}}{k_f}\Theta'(0)$	$\frac{-k_{nf}}{k_f}\Theta'(0)$
0.00	1.770948	1.770948	1.77094791
0.50	1.725631	1.725631	1.72563892
1.00	1.660286	1.660286	1.66028591
2.00	1.533487	1.533487	1.53348701

4. Results and discussion

Equations (9) and (12) subject to the boundary conditions, Eq. (13), are solved numerically using the Lobatto III A (Runge-Kutta) method in MATLAB. The impact of relevant factors, to be precise Ri, A, B, Sc, ϕ, etc. on the velocity, mass and heat transfer of the rotatory flow over an elongated sheet are discussed. The non-dimensional parameter values such as Ri = 0.2, $R_0 = 0.02$, $\phi = 0.05$, Sc = 0.5, $A = 0.2$ and $B = 0.3$ are kept as common in the entire analysis unless stated otherwise.

The effect of the Richardson number (Ri) and the rotation parameter R_0 on the profiles of primary and secondary velocities as well as on the temperature and concentration of the Cu-water nanofluid is observed in Figs. 2 to 5. It is evident from the figures that the amplified values of Ri improve the primary velocity gradient $F'(\eta)$, whereas the secondary velocity gradient $G(\eta)$, thermal and concentration boundary layers exhibit the opposite behaviour. These oscillations in secondary velocity gradient, resulting from the angular momentum's excess convection, occurred in the boundary layer's physical space.

The primary velocity layer diminishes with magnification in rotational parameter R_0 as displayed in Fig 2. With rising in R_0, the profile of the secondary velocity gradient takes an S-shape as illustrated in Fig 3. This occurs as a result of the Coriolis force, which when the moving plate is suddenly set in motion, acts as a constraint in the primary fluid flow. It is possible to state that the Coriolis force stopped fluid flow in the primary flow direction to create a secondary and cross flows in the flow field [33]. Figures 4 and 5 depict that growth in R_0 leads to the increase in $\Theta(\eta)$ and $\Phi(\eta)$ profiles.

For the positive values of A and B, as demonstrated in Fig. 6, the magnification of the space and time-dependent non-uniform heat source/sink leads to the enhancement of the primary velocity gradient and fall in profiles of the secondary velocity.

The temperature rises as A and B increase, as shown in Fig. 7. The height of the concentration boundary layer decreases when A and B increase, as seen in Fig. 8. Physically these effects

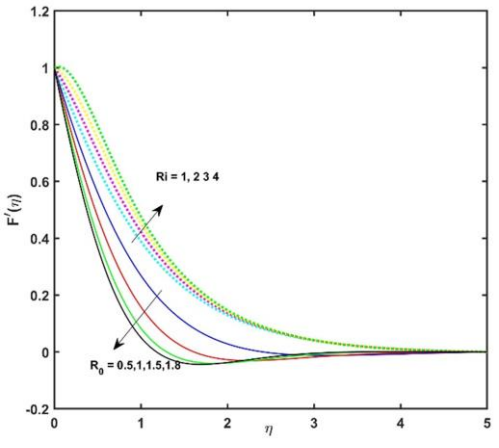

Fig. 2. Impact of rotation parameter (R_0) and Richardson parameter (Ri) on $F'(\eta)$.

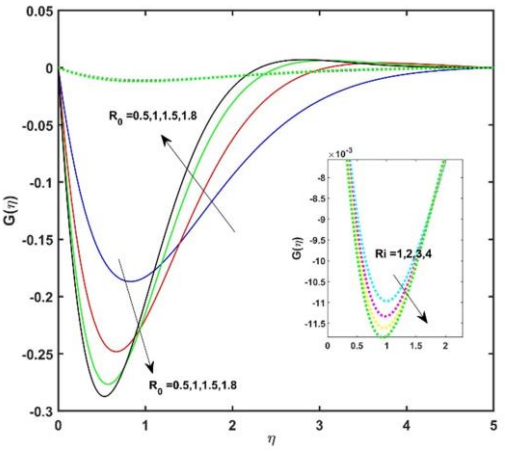

Fig. 3. Impact of R_0 and Ri on $G(\eta)$.

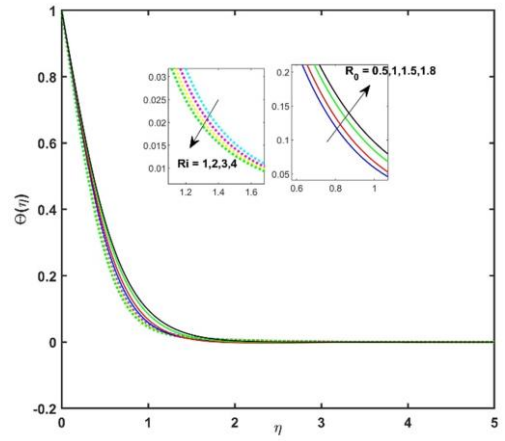

Fig. 4. Impact of R_0 and Ri on $\Theta(\eta)$.

can be related to the fact that the growth in the values of A and B prominently rises the temperature of the nanofluid, and the nanoparticles diffuse from higher to lower thermal areas, lowering the concentration boundary layer.

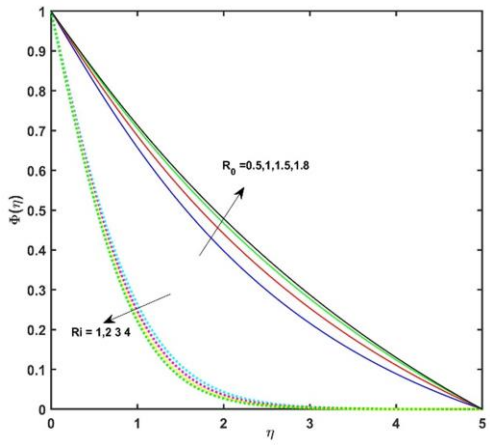

Fig. 5. Impact of R_0 and Ri on $\Phi(\eta)$.

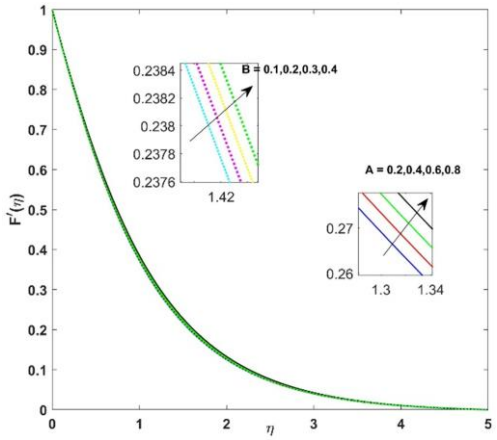

Fig. 6. Impact of A and B on $F'(\eta)$.

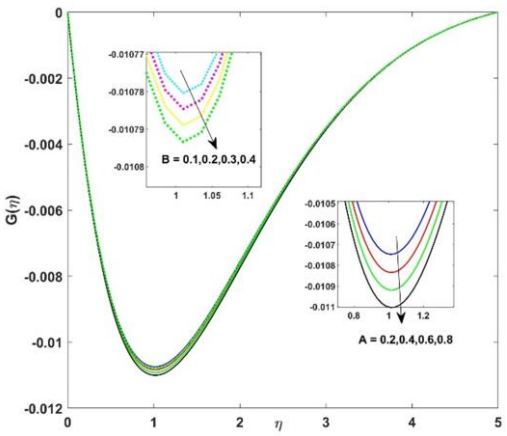

Fig. 7. Impact of A and B on $G(\eta)$.

Figure 9 displays the impact of time and spatial reliable heat sources on the concentration profile. We observe that the concentration boundary layer of the nanoparticles decreases with an increase in values of A and B. Figure 10 displays the effect of Cu-nanoparticle volume fraction (ϕ) change on the physical parameters of the rotating flow. As the values of ϕ escalate, the primary velocity and concentration of species fall. Moreover, increasing the volume percent of nanoparticles increases the thermal conductivity, the secondary velocity gradient, and thermal boundary layer. This is because the volume density of nanofluids increases with the volume fraction of nanoparticles, slowing the flux of nanofluids, thickening the thermal boundary layer, increasing the thermal conductivity and accelerating the surface heat transfer coefficient [34].

The 'molecular diffusivity' deteriorates as the Schmidt number develops and the concentration boundary layer shrinks, as exhibited in Fig. 11.

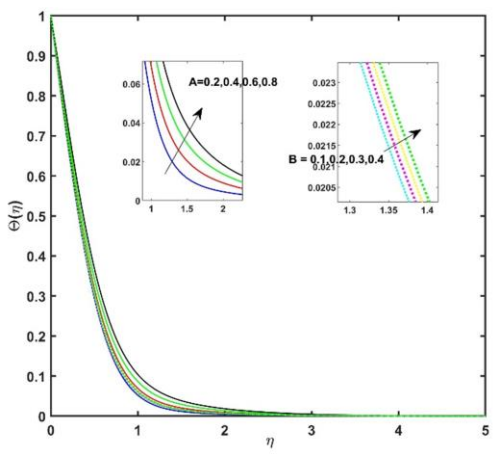

Fig. 8. Impact of A and B on $\Theta(\eta)$.

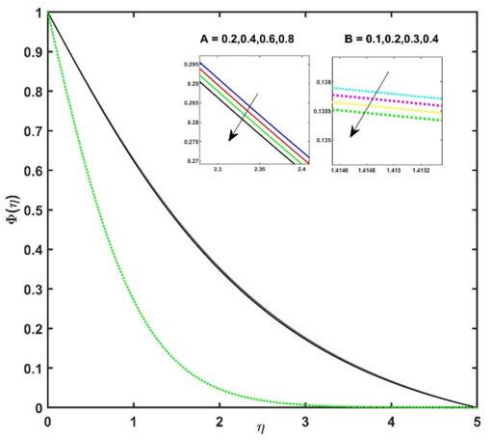

Fig. 9. Impact of A and B on $\Phi(\eta)$.

From Table 4 we observe that the production of thermal energy increases as A and B increase. As a result, the nanofluid temperature rises, causing the Nusselt number to decrease and drop, while the Sherwood number tends to rise. With the increase in Sc, the Nusselt number decreases, and the Sherwood

Table 4. The calculated values of C_{fx}, C_{fy}, $-\frac{k_{nf}}{k_f}\theta'(0)$ and $-\frac{1}{1-\phi}\phi'(0)$ for different values of the physical parameters.

Parameter	$\frac{\mu_{nf}}{\mu_f}f''(0)$	$\frac{\mu_{nf}}{\mu_f}g'(0)$	$Re_x^{-1/2}Nu_x$	$Re_x^{-1/2}Sh_x$	Parameter	$\frac{\mu_{nf}}{\mu_f}f''(0)$	$\frac{\mu_{nf}}{\mu_f}g'(0)$	$Re_x^{-1/2}Nu_x$	$Re_x^{-1/2}Sh_x$
R_0 = 0.0	-1.0114290	0.0000000	1.8681770	0.4433540	B = 0.1	-1.0165690	-0.0412950	1.9697570	0.3898610
R_0 = 1.0	-1.5410230	-1.4232460	1.7145830	0.3827830	B = 0.2	-1.0118770	-0.0413400	1.9175650	0.3903580
R_0 = 1.5	-1.8342400	-1.8399630	1.5827540	0.3620820	B = 0.3	-1.0070340	-0.0413870	1.8643150	0.3908740
R_0 = 1.8	-1.9978780	-2.0498870	1.4998280	0.3528740	B = 0.4	-1.0020290	-0.0414360	1.8099550	0.3914080
Ri = 0.5	-1.0070340	-0.0413870	1.8643150	0.3908740	φ = 0.0	-0.7324850	-0.0249520	1.7003820	0.4301090
Ri = 1.0	-0.5236630	-0.0434250	1.9352600	0.4133410	φ = 0.1	-0.7898190	-0.0279390	1.7360860	0.4309590
Ri = 2.0	-0.0665240	-0.0450680	1.9952570	0.4318640	φ = 0.3	-0.8458140	-0.0309340	1.7710520	0.4327930
Ri = 2.5	0.3710150	-0.0464600	2.0477770	0.4477820	φ = 0.5	-0.9011610	-0.0339670	1.8049780	0.4355000
A = 0.2	-1.0237050	-0.0400830	1.9513770	0.4421270	Sc = 0.0	-1.0070340	-0.0413870	1.8643150	0.3908740
A = 0.4	-0.9999550	-0.0404290	1.7839950	0.4444610	Sc = 0.3	-1.0070340	-0.0413870	1.8643150	0.6329460
A = 0.6	-0.9757630	-0.0407730	1.6134640	0.4468200	Sc = 0.5	-1.0070340	-0.0413870	1.8643150	0.8261700
A = 0.8	-0.9511620	-0.0411140	1.4398230	0.4491990	Sc = 0.6	-1.0070340	-0.0413870	1.8643150	0.9892370

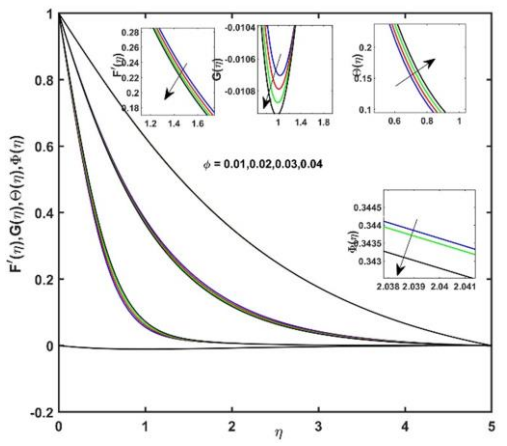

Fig. 10. Impact of Φ on $F'(\eta)$, $G(\eta)$, $\Theta(\eta)$ and $\Phi(\eta)$.

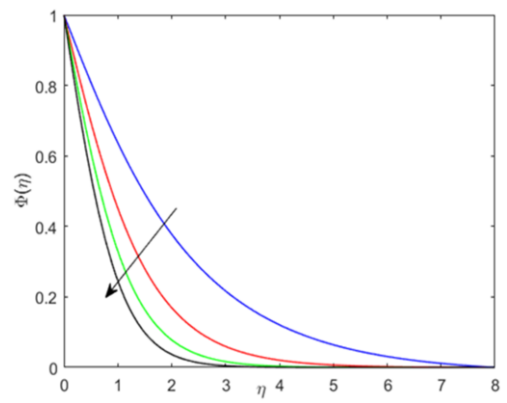

Fig. 11. Impact of Sc on $\Phi(\eta)$.

number increases. The higher the Sc, the lower the molecule diffusivity and the smaller the concentration boundary layer.

The improvement in the values of Ri and ϕ leads to the enrichment of the Nusselt number and the mass diffusivity coefficient. On the other hand, their enlargement results in the drop of primary and secondary drag friction values as shown in Table 4.

5. Conclusions

This study concentrated on the impacts of convection, uneven heat production and uneven heat absorption on the rotating flow of Cu-water nanofluid. In order to assess several properties, such as velocity, mass and heat transfer, we performed mathematical evaluations of the governing equations. The results we obtained are beneficial. These estimations, which were derived over a broad range of parameter values, provide a thorough grasp of the system under study.

The key observations after an intensive and integrated mathematical study are:

- The velocity, temperature and concentration boundary layers are significantly impacted by the Coriolis force. Secondary flow patterns are created as a result of the velocity boundary layer's deflection and deviation. The Coriolis force affects temperature gradients and can lead to the creation of thermal anomalies in thermal boundary layers. Similar to this, the Coriolis force influences solute transport in the concentration boundary layer, causing mixing and changing concentration distributions. The precise effect of the Coriolis force on these boundary layers relies on a number of variables, including the strength of force, the strength of flow and interactions with other forces in the system.
- Richardson's number governs the balance between buoyancy and other forces (inertia, thermal diffusion or diffusion) in the velocity, heat and concentration boundary layers. It determines the thickness, turbulence and heat or mass transfer properties of these boundary layers. The specific effect of Richardson's number on each boundary layer depends on the specific flow conditions and the relative importance of different forces in the system.
- Nu and Sh values both increase when copper nanoparticles are added to base fluids. It increases Nu to increase the efficiency of heat transmission and Sh to increase the efficiency of mass transfer. These outcomes are advantageous for many technical applications that need for effective mass and heat transport.

- Skin friction increases with rising Schmidt number, volume fraction parameter and heat source values.
- Under the impact of the forces at play, the nanoparticles in the range of parameters examined neither settle nor separate from the primary nanofluid. They may be mixed and displaced, yet they stay suspended.

References

[1] Ragupathi, P., Hakeem, A.K.A., Al-Mdallal, Q.M., Ganga, B., & Saranya, S. (2019). Non-uniform heat source/sink effects on the three-dimensional flow of Fe_3O_4/Al_2O_3 nanoparticles with different base fluids past a Riga plate. *Case Studies in Thermal Engineering*, 15, 100521. doi: 10.1016/j.csite.2019.100521

[2] Hyder, A., Lim, Y. J., Khan, I., & Shafie, S. (2023). Unveiling the performance of Cu-water nanofluid flow with melting heat transfer, MHD, and thermal radiation over a stretching/shrinking sheet. *ACS Omega*, 32(8), 29424–29436.

[3] Iftikhar, N., Rehman, A., & Sadaf, H. (2021). Theoretical investigation for convective heat transfer on Cu/water nanofluid and (SiO_2-copper)/water hybrid nanofluid with MHD and nanoparticle shape effects comprising relaxation and contraction phenomenon. *International Communications in Heat and Mass Transfer*, 120, 105012. doi: 10.1016/j.icheatmasstransfer.2020.105012

[4] Hazarika, S., Ahmed, S., & Yao, S.-W. (2023). Investigation of Cu-water nano-fluid of natural convection hydro-magnetic heat transport in a Darcian porous regime with diffusion-thermo. *Applied Nanoscience*, 13(1), 283–293. doi: 10.1007/s13204-020-01655-w

[5] Uddin, M.J., & Rasel, S.K. (2019). Numerical analysis of natural convective heat transport of copper oxide-water nanofluid flow inside a quadrilateral vessel. *Heliyon*, 5(5), e01757. doi: 10.1016/j.heliyon.2019.e01757

[6] Babu, R.S., Kumar, B.R., & Makinde, O.D. (2018). Chemical reaction and thermal radiation effects on MHD mixed convection over a vertical plate with variable fluid properties. *Defect and Diffusion Forum*, 387, 332–342. doi: 10.4028/www.scientific.net/DDF.387.332

[7] Yacob, N.A., Dzulkifli, N.F., Salleh, S.N.A., Ishak, A., & Pop, I. (2022). Rotating flow in a nanofluid with CNT nanoparticles over a stretching/shrinking surface. *Mathematics*, 10(1), 7. doi: 10.3390/math10010007

[8] Mehrez, Z., El Cafsi, A., Belghith, A., & Le Quéré, P. (2015). MHD effects on heat transfer and entropy generation of nanofluid flow in an open cavity. *Journal of Magnetism and Magnetic Materials*, 374, 214–224. doi: 10.1016/j.jmmm.2014.08.010

[9] Punith Gowda, R.J., Naveen Kumar, R., Jyothi, A.M., Prasannakumara, B.C., & Sarris, I.E. (2021). Impact of binary chemical reaction and activation energy on heat and mass transfer of Marangoni driven boundary layer flow of a non-Newtonian nanofluid. *Processes*, 9(4), 702. doi: 10.3390/pr9040702

[10] Shahzad, F., Jamshed, W., Sajid, T., Nisar, K.S., & Eid, M.R. (2021). Heat transfer analysis of MHD rotating flow of Fe_3O_4 nanoparticles through a stretchable surface. *Communications in Theoretical Physics*, 73(7), 75004. doi: 10.1088/1572-9494/abf8a1

[11] Ashraf, M., Ullah, Z., Zia, S., Alharbi, S.O., Baleanu, D., & Khan, I. (2021). Analysis of the physical behavior of the periodic mixed-convection flow around a nonconducting horizontal circular cylinder embedded in a porous medium. *Journal of Mathematics*, 2021(1), 8839146. doi: 10.1155/2021/8839146

[12] Ullah, Z., Akkurt, N., Alrihieli, H.F., Eldin, S.M., Alqahtani, A.M., Hussanan, A., et al. (2022). Temperature-dependent density and magnetohydrodynamic effects on mixed convective heat transfer along magnetized heated plate in thermally stratified medium using Keller box simulation. *Applied Sciences*, 12(22), 11461. doi: 10.3390/app122211461

[13] Khan, M.N., & Nadeem, S. (2020). Theoretical treatment of bioconvective Maxwell nanofluid over an exponentially stretching sheet. *Canadian Journal of Physics*, 98(8), 732–741. doi: 10.1139/cjp-2019-0380

[14] Khan, M.N., Hussien, M.A., Allehiany, F.M., Ahammad, N.A., Wang, Z., & Algehyne, E.A. (2023). Variable fluid properties and concentration species analysis of a chemically reactive flow of micropolar fluid between two plates in a rotating frame with cross diffusion theory. *Tribology International*, 189, 108943. doi: 10.1016/j.triboint.2023.108943

[15] Khan, M.N., Ahmad, S., Alrihieli, H.F., Wang, Z., Hussien, M. A., & Afikuzzaman, M. (2023). Theoretical study on thermal efficiencies of Sutterby ternary-hybrid nanofluids with surface catalyzed reactions over a bidirectional expanding surface. *Journal of Molecular Liquids*, 391 B, 123412. doi: 10.1016/j.molliq.2023.123412

[16] Sathyanarayana, M., & Goud, T.R. (2023). Numerical study of MHD Williamson-nano fluid flow past a vertical cone in the presence of suction/injection and convective boundary conditions. *Archives of Thermodynamics*, 44(2), 115–138. doi: 10.24425/ather.2023.146561

[17] Madhusudhana Rao, B., Gopal D., Kishan N., Ahmed Saad, & Durga Prasad P. (2020). Heat and mass transfer mechanism on three-dimensional flow of inclined magneto Carreau nanofluid with chemical reaction. *Archives of Thermodynamics*, 41(2), 223–238. doi: 10.24425/ather.2020.133630

[18] Das, S., Jana, N.R., & Makinde, O.D. (2014). MHD boundary layer slip flow and heat transfer of nanofluid past a vertical stretching sheet with non-uniform heat generation/absorption. *International Journal of Nanoscience*, 13(3), 1–12. doi: 10.1142/S0219581X14500197

[19] Oke, A.S., Prasannakumara, B.C., Mutuku, W.N., Gowda, R.J. P., Juma, B.A., Kumar, R.N., & Bada, O.I. (2022). Exploration of the effects of Coriolis force and thermal radiation on water-based hybrid nanofluid flow over an exponentially stretching plate. *Scientific Reports*, 12, 21733. doi: 10.1038/s41598-022-21799-9

[20] Owhaib, W., Basavarajappa, M., & Al-Kouz, W. (2021). Radiation effects on 3D rotating flow of Cu-water nanoliquid with viscous heating and prescribed heat flux using modified Buongiorno model. *Scientific Reports*, 11, 20669. doi: 10.1038/s41598-021-00107-x

[21] Ragulkumar, E., Palani, G., Sambath, P., & Chamkha, A.J. (2023). Dissipative MHD free convective nanofluid flow past a vertical cone under radiative chemical reaction with mass flux. *Scientific Reports*, 13, 2878. doi: 10.1038/s41598-023-28702-0

[22] Jalili, P., Sadeghi Ghahare, A., Jalili, B., & Domiri Ganji, D. (2023). Analytical and numerical investigation of thermal distribution for hybrid nanofluid through an oblique artery with mild stenosis. *SN Applied Sciences*, 5(95). doi: 10.1007/s42452-023-05312-z

[23] Farrukh, B.M., Chen, G.M., & Tso, C.P. (2021). Viscous dissipation effect on CuO-water nanofluid-cooled microchannel heat sinks. *Case Studies in Thermal Engineering*, 26, 101159. doi: 10.1016/j.csite.2021.101159

[24] Sheikholeslami, M., Ashorynejad, H.R., Domairry, G., & Hashim, I. (2012). Flow and heat transfer of Cu-water nanofluid between a stretching sheet and a porous surface in a rotating system. *Journal of Applied Mathematics*, 2012(1), 421320. doi: 10.1155/2012/421320

[25] Hayat, T., Imtiaz, M., & Alsaedi, A. (2016). Melting heat transfer in the MHD flow of Cu–water nanofluid with viscous dissipation and Joule heating. *Advanced Powder Technology*, 27(4), 1301–1308. doi: 10.1016/j.apt.2016.04.024

[26] Owhaib, W., Basavarajappa, M., & Al-Kouz, W. (2021). Radiation effects on 3D rotating flow of Cu-water nanoliquid with viscous heating and prescribed heat flux using modified Buongiorno model. *Scientific Reports*, 11(1), 20669. doi: 10.1038/s41598-021-00107-x

[27] Triveni, B., Rao, M. V.S., Gangadhar, K., & Chamkha, A.J. (2023). Heat transfer analysis of MHD Casson nanofluid flow over a nonlinear stretching sheet in the presence of nonuniform heat source. *Numerical Heat Transfer, Part A: Applications*, 85(13), 2145–2164. doi:10.1080/10407782.2023.2219831

[28] Khan, U., Zaib, A., Khan, I., & Nisar, K. S. (2020). Activation energy on MHD flow of titanium alloy (Ti6Al4V) nanoparticle along with a cross flow and streamwise direction with binary chemical reaction and non-linear radiation: Dual solutions. *Journal of Materials Research and Technology*, 9(1), 188–199. doi: 10.1016/j.jmrt.2019.10.044

[29] Aybar, H., Sharifpur, M., Azizian, M.R., Mehrabi, M., & Meyer, J.P. (2015). A review of thermal conductivity models for nanofluids. *Heat Transfer Engineering*, 36(13), 1085–1110. doi: 10.1080/01457632.2015.987586

[30] Gamaoun, F., Ullah, Z., Ameer Ahammad, N., Fadhl, B.M., Makhdoum, B.M., & Abbas Khan, A. (2023). Effects of thermal radiation and variable density of nanofluid heat transfer along a stretching sheet by using Keller box approach under magnetic field. *Thermal Science and Engineering Progress*, 41, 101815. doi: 10.1016/j.tsep.2023.101815

[31] Prathiba, A., & Akavaram, V.L. (2022). Numerical investigation of a convective hybrid nanofluids around a rotating sheet. *Heat Transfer*, 51(4), 3353–3372. doi: 10.1002/htj.22454

[32] Hayat, T., Nadeem, S., & Khan, A.U. (2020). Aspects of 3D rotating hybrid CNT flow for a convective exponentially stretched surface. *Applied Nanoscience*, 10(8), 2897–2906. doi: 10.1007/s13204-019-01036-y

[33] Mohd Zin, N.A., Khan, I., Shafie, S., & Alshomrani, A.S. (2017). Analysis of heat transfer for unsteady MHD free convection flow of rotating Jeffrey nanofluid saturated in a porous medium. *Results in Physics*, 7, 288–309. doi: 10.1016/j.rinp.2016.12.032

[34] Abbas, W., & Magdy, M.M. (2020). Heat and mass transfer analysis of nanofluid flow based on Cu, Al2O3, and TiO2 over a moving rotating plate and impact of various nanoparticle shapes. *Mathematical Problems in Engineering*, 2020. doi: 10.1155/2020/9606382